CONF-881151--62

CONF-881151--62

DE89 011574

## DISCLAIMER

curves. Hence, rather direct methods can be used to study electron correlation in slow, multicharged collision systems.

The system $O^{6+}$+He has received much attention with regard to electron correlation effects[10-18]. In this system correlated and uncorrelated double electron transitions populate different final states which can be measured separately[10]. The uncorrelated double capture which involve two sequential one-electron transitions creates the configurations $1s^2 3\ell 3\ell'$ (or $1s^2 3\ell 4\ell'$) of *equivalent* (or nearly equivalent) electrons. (Hereafter the $1s^2$ core is not indicated in the configurations.) On the other hand, the correlated double capture process produce the *nonequivalent* electron configurations $2pn\ell$ as a result of energy exchange between the transferred electrons. The states attributed to the equivalent and nonequivalent configurations decay by autoionization producing L-Auger and Coster-Kronig electrons, respectively. The important point is that the ejected electrons, which are a signature of uncorrelated and correlated double capture, can be distinguished using high-resolution electron spectroscopy.

In this work experiments of Coster-Kronig transitions in slow ion-atom collisions are reviewed with regard to recent critical considerations of correlation effects in the 60-keV $O^{6+}$+He system[5,12,19,20]. Electron correlation is found to be significant in various mechanisms of two-electron transfer. To support the present conclusions, calculations are made applying realistic two-electron matrix elements within the framework of the Landau-Zener model. Our experimental results were partially discussed in previous articles[14,15,17]. More general aspects of the present theoretical work can be found in a recent review[21] dealing with electron correlation effects in ion-atom collisions.

## 2. Discussion of Experimental Results

The present measurements of the Coster-Kronig and Auger electron spectra were performed using the zero-degree spectroscopy method described elsewhere[22]. It is noted that our previous measurements[10] of the $O^{6+}$+He system were performed utilizing an electron acceleration method which may have spuriously enhanced the electron intensities. Recently we re-measured part of our data without using the acceleration method[17]. Results for the system 60-keV $O^{6+}$+He are given in Fig. 1 showing Coster Kronig lines

associated with the configurations $2pn\ell$ with $n\geq 6$ and Auger lines due to the configurations $3\ell n\ell'$ with $n\geq 3$. The new data confirm the previous Coster-Kronig line intensities[10] within the experimental uncertainties. The $O^{6+}$+He system yields the considerable value of ~0.3 for the fraction of the Coster Kronig line intensity relative to the total (Auger and Coster-Kronig) line intensity. This fraction corresponds to the cross section $\sigma_{2pnl} = 9\times10^{-17}$ cm$^2$ for the production of all configurations $2pn\ell$[14,17]. The cross sections for the individual configurations (e.g. $2p6\ell$) are plotted in Fig. 2. Inspection of the data shows that the cross sections follow the well-known $n^{-3}$ law.

From the line intensities of the Coster-Kronig electrons it was concluded that correlation effects play a significant role in double capture for 60-keV $O^{6+}$+He collisions[10]. This conclusion has also been drawn for other slow, multicharged collision systems[14,17]. However, the magnitude of the correlation effects has become a matter of controversy[12,13].Our $O^{6+}$+He data[10,17] for the relative Coster-Kronig line intensities agree with those measured by Mann and Schulte[11], but they are larger by a factor of ~5 than the results obtained by Mack and Niehaus[9] and Bordenave-Montesquieu et al.[16]. It may be anticipated that anisotropic angular distributions may partially be responsible for the observed discrepancies[13], but this supposition could not be substantiated[17]. It appears that instrumental effects, which often disturb the measurements of low-energy electrons, are responsible for the observed discrepancies. It should be added that very recent results by Chartrenne et al.[23] confirm our data[10,17] for the relative Coster-Kronig line intensities.

To obtain information about the population of the angular momenta $\ell$ in the Coster-Kronig configurations $2pn\ell$, measurements with high resolution were performed[18]. The line structure associated with the configurations $2p6\ell$ is plotted in Fig. 3. It is seen that the line intensities due to the low angular momenta $\ell$=0 and 1 are rather weak. The maximum intensity is attributed to the high angular momenta $\ell\geq 3$. This finding has been explained by the possibility that not only energy but also angular momentum is exchanged between the two electrons involved in the double capture process[18]. When one electron is transferred to the 2p orbital it is likely to lose angular momentum which is given to the electron transferred to the $n\ell$ level. Hence, the high values of the angular momentum in the $2pn\ell$ configurations may partially be understood.

## 3. Mechanisms for Double Electron Capture

Electron correlation processes in slow ion–atom collisions can be verified by means of crossings of potential curves representing multi-electron states[15,17]. Fig. 4 shows the potential curves for a limited number of molecular $(OHe)^{6+}$ states relevant for the production of the equivalent $3d^2$ and nonequivalent $2p6\ell$ electron configurations. Crossings between potential curves which differ by one spin orbital (circles) and two spin orbitals (squares) are denoted as Diabatic I and II, respectively[24]. In the crossing of type I, transitions are caused by a one-electron interaction such as radial coupling, whereas a transition at a crossing of type II requires a two-electron interaction such as electron correlation.

Each process affecting two electrons may in principle be produced by one correlated transition or by two independent single-electron transitions[19]. Accordingly, the potential curves involved in these transitions form a 'reaction triangle' whose corners refer to two crossings of type I (circles) and one crossing of type II (square). Two such 'triangles' are indicated by hatched areas in Fig. 4. It is seen that the 'triangle' N associated with the nonequivalent configurations $2p6\ell$ is considerably larger than the 'triangle' E attributed to the equivalent configuration $3d^2$. These diagrams illustrate that there are striking differences in the production of nonequivalent and equivalent electron configurations in $O^{6+}$+He collisions.

Inspection of the 'triangle' E suggests that the single-electron transitions are significant for the production of the configuration $3d^2$. In this case the question of whether the correlated two-electron transitions are also significant has not as yet been discussed in detail. It is interesting to note that Barat and collaborators[19], who studied the system $O^{8+}$+He, have found negligible electron correlation effects in the population of equivalent (or nearly equivalent) electron configurations. However, this conclusion is not necessarily valid for the $O^{6+}$+He system. It is noted that Mack et al.[25] recently observed electron correlation effects in $C^{6+}+H_2$ collisions producing the equivalent $3\ell3\ell'$ configurations.

In any case, it cannot be concluded that uncorrelated single-electron transitions are dominant for the nonequivalent configurations $2pn\ell$. It is pointed out that in their previous work Barat and collaborators[19] did not

consider the significant difference in the production of the *equivalent* and *nonequivalent* electron configurations. For the case of the nonequivalent configurations 2pn$\ell$, which are associated with the 'triangle' N, the potential curves already qualitatively indicate that the uncorrelated single-electron transitions are not important (Fig. 4). In fact, the curves attributed asymptotically to $O^{6+}$+He($1s^2$) and $O^{5+}(6\ell)$+$He^{+}$(1s) do not even cross. Similarly, it is not expected that the state labeled $O^{5+}$(2p)+$He^{+}$(1s) contributes much to the production of the 2p6$\ell$ configurations. Accordingly, Rongin et al.[20] recently confirmed that two successive single-electron transitions are not responsible for the production of the 2pn$\ell$ configuration in the $O^{6+}$+He system. Instead it is anticipated that correlation effects play a role.

The correlated double capture (CDC) process considered previously[10] corresponds to the crossing which is seen near the square at 3.8 a.u formed by the incident horizontal curve and the curve labeled asymptotically $O^{4+}$(2p6$\ell$)+$He^{2+}$. Winter et al.[12] pointed out another process which can produce the 2pn$\ell$ configurations. This process involves a single-electron transition into the state labeled $O^{5+}$(3d)+$He^{+}$(1s) near 4.3 a.u. followed by a correlated transfer (de)excitation (CTE) process populating the final $O^{4+}$(2p6$\ell$)+$He^{2+}$ state near 3.5 a.u. Thus, double electron capture into the 2pn$\ell$ configurations may proceed via a *one-step* process and a *two-step* process, both involving electron correlation effects. Hence, it is noted that the occurrence of a successive two-step process is by no means an indication for the absence of electron correlation. For instance, at relatively small impact energies Rongin et al.[20] found strong evidence for the two-step process[12] but they confirmed also electron correlation effects in the production of the 2pn$\ell$ configurations.

In addition to the mechanisms associated with the 'triangle' N, one may consider a correlated transfer (target) excitation process[21] producing the 2pn$\ell$ configurations. Near 2 a.u. this process occurs as the transfer of a helium electron to the oxygen 2p level and the excitation of the other helium electron into, e.g., n=4 which may subsequently be transferred to the 6$\ell$ level of oxygen (Fig. 4). In the following we shall focus our attention on the processes CDC and CTE which are quite similar, since they are close in distance and they have in common the correlated two-electron transition populating directly the 2pn$\ell$ configurations. It should be added that both CDC and CTE have been known for several years, e.g., they have been studied by Kimura and Olson[4] and by Kimura et al.[26], respectively.

## 4. Calculations for Double Electron Capture

To support the conclusions of the previous discussion, theoretical estimates are made to obtain quantitative information about the different mechanisms involved in the production of the nonequivalent configurations $2pn\ell$. The calculations are based on the well-known cross section formula

$$\sigma = P \pi R_c^2 \qquad (1)$$

which is valid for transitions at localized crossings occurring with the probability P at the radius $R_c$. In the following we shall focus our attention on the cross section $\sigma_{2p6l}$ for the production of the configurations $2p6\ell$. It will be shown that the contribution from the successive single-electron transitions is small and that the theoretical cross sections obtained for the correlated processes CDC and CTE are consistent with the experimental data.

In the case of two *independent* capture events the probability P is obtained as a product of the single-electron transition probabilities attributed to the inner and outer crossing. The distance $R_c$ is taken to be equal to the smaller crossing radius. Unfortunately, suitable data for the single-electron transitions populating the 2p and $6\ell$ levels of $O^{6+}$ (or $O^{7+}$) in collisions with He are not available at present. However, extrapolated single-capture data by Gordeev et al.[27] and Barat et al.[19] strongly suggest that the independent single-electron transitions are not significant in the production of the $2p6\ell$ configurations. This conclusion is supported by recent results obtained from the extended over-barrier model by Niehaus[28] neglecting electron correlation effects. It was found that the ratio of cross sections[28] for the production of the $2p6\ell$ and $3d^2$ configurations is less than 0.01, which is more than an order of magnitude smaller than the experimental value of 0.3 mentioned above. Better agreement with the present data is obtained from a modified version of the model[29] allowing for energy exchange between the captured electrons, which means that some correlation between the electrons is included in the analysis.

It thus appears that the production of the non-equivalent configurations $2pn\ell$ involves electron correlation. To obtain theoretical results for the CDC and CTE processes, estimates of the related cross sections are made by means of the Landau-Zener formula[30]. This formula yields the following approxi-

mate relation for small transition probabilities[15]:

$$P = 8\pi \frac{|V_{1f}^{c}|^2}{Fv} \qquad (3)$$

where $V_{1f}^{c}=\langle\Phi_f|r_{12}^{-1}|\Phi_i\rangle$ is the correlation matrix element with the distance $r_{12}=|\vec{r}_1-\vec{r}_2|$ between the electrons, v is the collision velocity, and F is the derivative of the energy difference of the associated diabatic potential curves at the crossing radius $R_c$. The crossing region is assumed to be passed twice and the radial velocity, which is usually applied in the Landau-Zener model[30], is set equal to half the incident velocity.

To apply eq. (3) the major work lies in the determination of the correlation matrix element $V_{1f}^{c}$. Fritsch[31] has calculated the matrix elements

$$\langle\varphi_{2p}\varphi_{6l}|r_{12}^{-1}|\varphi'_{1s}\varphi'_{1s}\rangle \qquad (4a) \qquad \text{and} \qquad \langle\varphi_{2p}\varphi_{6l}|r_{12}^{-1}|\varphi'_{1s}\varphi_{3d}\rangle \qquad (4b)$$

with the atomic 1s orbital $\varphi'_{1s}$ centered at the target and the atomic orbitals $\varphi_{2p}$, $\varphi_{3d}$, and $\varphi_{6l}$ centered at the projectile. For $R_c$=3.8 a.u., the matrix elements were determined to be within the range of 2 - $4\times10^{-3}$ a.u. depending on the angular momentum $\ell$. The data set is based on atomic orbitals coupled to the magnetic quantum number M=0 of the total angular momentum Additional calculations showed that the overlap matrix elements due to the non-orthogonality of the wave functions are negligible[31].

Let us first consider the CDC process[10]. It refers to the crossing of the incident state starting with $O^{6+}$+He($1s^2$) and the state attributed asymptotically to $O^{4+}(2p6\ell)+He^{2+}$ as noted above. For this crossing one obtains F=0.56 a.u. Also it follows for 60-keV $O^{6+}$ that v=0.39 a.u. With the matrix elements by Fritsch[31] one obtains theoretical transition probabilities of ~$6\times10^{-4}$, which yields the cross section of ~$2\times10^{-18}$ $cm^2$. To compare this value with the experimental data of $2.8\times10^{-17}$ $cm^2$ (Fig. 2) it should be taken into account that numerous (i.e. 36) angular momenta[18] and magnetic quantum numbers may contribute to the cross section $\sigma_{2p6l}$. The sum of about 15 similar contributions would yield the experimental results.

Recently, Fritsch[31] calculated CDC cross sections summed over all final angular momenta for the 40-keV $C^{6+}$+He system whose impact velocity and

potential curve structures are nearly equal to those of the 60-keV $O^{6+}$+He system. The calculated cross sections[31] for the production of the $2p6\ell$ configurations range from 1.2 to $3.6\times10^{-17}$ $cm^2$, depending on whether only M=0 or all M are taken into account. This shows that the calculations made under the assumption that CDC is producing the $2p6\ell$ configurations in 60-keV $O^{6+}$+He collisions are consistent with experiment.

Further theoretical effort is required to study the process of correlated transfer excitation, CTE[12]. It is noted that the matrix elements (4a) and (4b) which are responsible for CDC and CTE, respectively, are nearly equal. Hence, the competition between the two processes is not decided by the correlated transitions but it is governed by the preceding single-electron transition where a helium 1s electron is captured into an oxygen $3\ell$ level near 4.3 a.u. The probability for this transition cannot readily be calculated, since the interaction between the incident state $O^{6+}$+He($1s^2$) and the $O^{5+}$(3d)+He(1s) state is so strong that their coupling region extends into the crossings associated with the CDC and CTE processes. This can be concluded from the magnitude of the related coupling matrix element given by Olson and Salop[32]. Thus, due to the overlap of the coupling regions one may suspect that the $O^{5+}$+He system is a good candidate to study the individual contributions of CDC and CTE, since these contributions are expected to add coherently. Consequently, the electron correlation processes CDC and CTE appear to be quite similar in the $O^{6+}$+He system.

Ronçin et al.[20] performed coupled channel calculations neglecting the CDC contribution completely.They found that the CTE process[12] alone would account for their experimental results obtained at the relative low energy of 9 keV. Here, for 60 keV, we found that the CDC process is important. It is noted that at low collision energies, where the system behaves adiabatically, the state attributed to $O^{5+}$(3d)+$He^{+}$(1s) is populated with a relatively high probability and, thus, the dominance of the CTE process is likely. However, this supposition cannot readily be generalized. At higher incident energies such as 60 keV it is likely that the system passes the crossing near 4.3 a.u. more diabatically. In any case it is expected with regard to the near equality of the matrix elements (4a) and (4b) that the CDC and CTE processes occur with probabilities of the same order of magnitude. Further theoretical work is suggested to include both processes of correlated double capture, CDC, and correlated transfer excitation, CTE, in coupled channel calculations.

Acknowledgement.

We are indebted to Dr. M. Barat for clarifying discussions. We would like to thank W. Fritsch and A. Niehaus for providing us with unpublished data and for fruitful suggestions. Helpful comments on the manuscript by Vic Montemayor are greatfully acknowledged. This work was sponsored by a NATO Collaboration Research Grant and by the Office of Fusion Energy, U.S. Department of Energy, under the Contract No. DE-AC05-84OR21400 with Martin Marietta Energy System, Inc.

Figure Caption

Fig. 1. Spectrum of $L_1$-Coster-Kronig (CK) and L-Auger electrons produced in 60-keV $O^{6+}$+He collisions[17].

Fig. 2. Cross sections for the production of the Coster-Kronig configurations $1s^2 2pn\ell$. Also shown are theoretical results proportional to $n^{-3}$ and normalized to the experimental data for n=9, 10, and 11.

Fig. 3 High resolution spectrum of $1s^2 2p6\ell$ Coster Kronig electrons showing the first peak of the Rydberg series seen in Fig. 1. Also shown are calculated transition energies associated with the angular momentum $\ell$. The lengths of the bars represent statistical weights.

Fig. 4. Potential curve diagram for the system $O^{6+}$ + He. The data are obtained by methods used in Refs. [15] and [17] where also more complete sets of potential curves are given.

References

[1] D.H. Crandall, R.E. Olson, E.J. Shipsey, and J.C. Browne, Phys. Rev. Lett. 36 (1976) 858

[2] T.P. Grozdanov and R.K. Janev, J. Phys. B. 13 (1980) 3431

[3] S. Tsurubuchi, T. Iwai, Y. Kaneko, M. Kimura, N. Kobayashi, A. Matsumoto, S. Ohtani, K. Okuno, S. Takagi, and H. Tawara, J. Phys. B 15 (1982) L733

[4] M. Kimura and R.E. Olson, J. Phys. B 18 (1984) L713

[5] P. Ronçin, M. Barat, H. Laurent, J. Pommier, S. Dousson, and D. Hitz, J. Phys. B 17 (1984) L521

[6] H. Cederquist, L.H. Anderson, A. Barany, P. Hvelplund, H. Knudsen, E.H. Nielsen, J.O. Pedersen, and J. Sørensen, J. Phys. B 18 (1985) 3951

[7] A. Niehaus, J. Phys. B 19 (1986) 2925

[8] A. Bordenave-Montesquieu, P. Benoit-Cattin, A. Gleize, A.I. Marakchi, S. Dousson, and D. Hitz, J. Phys. B 17 (1984) L127 and L223

[9] M. Mack and A. Niehaus, Nucl. Instr. Meth. B23 (1987) 116

[10] N. Stolterfoht, C.C. Havener, R.A. Phaneuf, J.K. Swenson, S.M. Shafroth, and F.W. Meyer, Phys. Rev. Lett. 57 (1986) 74

[11] R. Mann and H. Schulte, Z. Physik D4 (1987) 343 and R. Mann, Phys. Rev. A 35 (1987) 4988

[12] H. Winter, M. Mack, R. Hoekstra, A. Niehaus, and F.J. de Heer, Phys. Rev. Lett. 58 (1987) 957

[13] N. Stolterfoht, C.C. Havener, R.A. Phaneuf, J.K. Swenson, S.M. Shafroth, and F.W. Meyer, Phys. Rev. Lett. 58 (1987) 958

[14] F.W. Meyer, C.C. Havener, R.A. Phaneuf, J.K. Swenson, S.M. Shafroth, and N. Stolterfoht, Nucl. Instr. Meth. B 24/25 (1987) 106

[15] N. Stolterfoht, C.C. Havener, R.A. Phaneuf, J.K. Swenson, S.M. Shafroth, and F.W. Meyer, Nucl. Instr. Meth. B 27 (1987) 584

[16] A. Bordenave-Montesquieu, P. Bernoit-Cattin, M. Boudjema, A. Gleizes, S. Dousson, amd D. Hitz, XVth ICPEC, Abstracts, edited by J. Geddes et al. (Belfast, 1987) p. 551 and 552

[17] F.W. Meyer, D.C. Griffin, C.C. Havener, N.S. Huq, R.A. Phaneuf, J.K. Swenson,and N. Stolterfoht, Electronic and Atomic Collisions, Invited Papers, edited by H.B. Gilbody, W.R. Newell, F.H. Read and A.C. Smith (North Holland, Amsterdam,1988) p. 673

[18] F.W. Meyer, D.C. Griffin, C.C. Havener, M.S. Huq, R.A. Phaneuf, J.K. Swenson, and N. Stolterfoht, Phys. Rev. Lett. 60 (1988) 1821

[19] M. Barat, M.N. Gaboriaud, L. Guillemot, P. Ronçin, and H. Laurent, J. Phys. B 20 (1987) 5571, H. Laurent, M. Barat, M.N. Gaboriaud, L. Guillemot,and P. Ronçin, J. Phys. B 20 (1987) 6581, and P. Ronçin, M. Barat, and H. Laurant, Europhys. Lett. 2 (1986) 371

[20] P. Ronçin, M. Barat, M.N. Gaboriaud, L. Guillemot, and H. Laurant, J. Phys. B, to be published

[21] N. Stolterfoht, Proceedings of the Conference of Spectroscopy and Collisions of Few Electron Ions (Central Institut of Physics, Bukarest, 1988) to be published

[22] A. Itoh, T. Schneider, G. Schiwietz, Z. Roller, H. Platten, G. Nolte, D. Schneider, and N. Stolterfoht, J. Phys. B 16 (1983) 3965

[23] S. Charlieenne, M. Prior, R. Bruch and D. Schneider, International Conference on the Physics of Multiply Charged Ions (Grenoble 1988) T.II.

[24] J.C. Brenot, D. Duicq, J.P. Guyacq, J. Pommier, V. Sidis, M. Barat, and E. Pollack, Phys. Rev. A 11 (1975) 1933

[25] M. Mack, J.H. Nijland, P.v.d. Straten, A. Niehaus, and R. Morgenstern, submitted to J. Phys. B (1988)

[26] M. Kimura, T. Iwai, Y. Kaneko, N. Kobayashi, S. Ohtani, K. Okuno, S. Takagi, H. Tawara, and Tsurubuchi, Phys. Rev. A. 26 (1982) 105

[27] Yu.S. Gordeev, D. Dijkkamp, A.G. Drentje, and F.J. de Heer, Phys. Rev. Lett. 50 (1983) 1842 and D. Dijkkamp, Yu.S. Gordeev, A. Brazku, A.G. Drentje, and F.J. De Heer, J. Phys B 18 (1985) 737

[28] A. Niehaus, private communication (1988)

[29] A. Niehaus, X-Ray and Inner-Shell Processes, edited by P. Lagarde, F.J. Wuilleumier, and J.P. Briand, J. Physique, Colloque C9 (1987) 137

[30] C.D. Landau, J. Phys. (USSR) 2 (1932) 46 and C. Zener, Proc. Roy Soc. A137 (1932) 696

[31] W. Fritsch, private communication (1987 and 1988)

[32] R.E. Olson and A. Salop, Phys. Rev. 14 (1976) 579

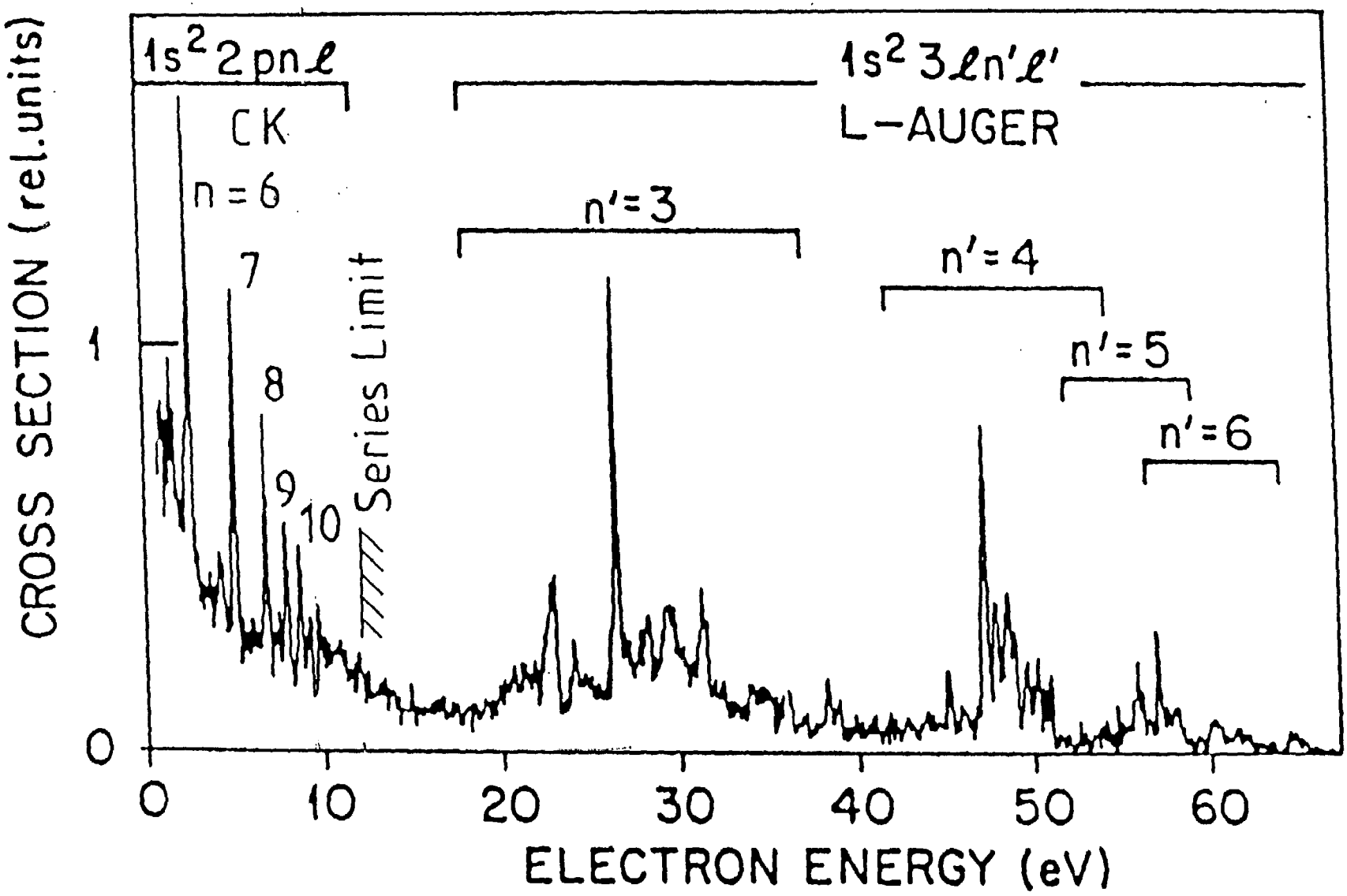
1s² 2pnℓ
CK
n = 6
7
8
9
10
Series Limit
1s² 3ℓn'ℓ'
L-AUGER
n'=3
n'=4
n'=5
n'=6
CROSS SECTION (rel.units)
1
0
0
10
20
30
40
50
60
ELECTRON ENERGY (eV)

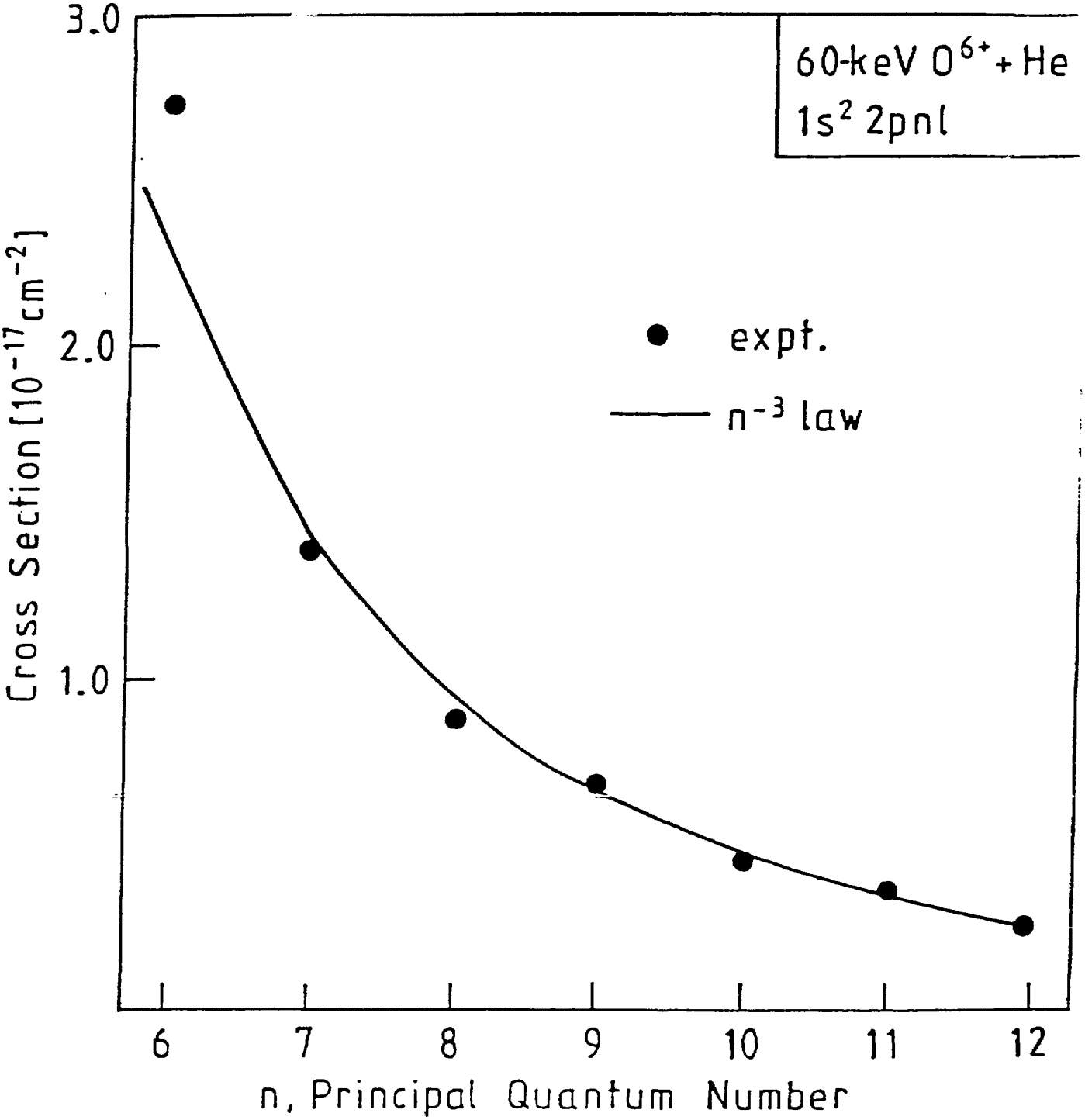
60-keV $O^{6+}$ + He
$1s^2$ 2pnl
expt.
$n^{-3}$ law
Cross Section [$10^{-17}$ $cm^{-2}$]
3.0
2.0
1.0
6
7
8
9
10
11
12
n, Principal Quantum Number

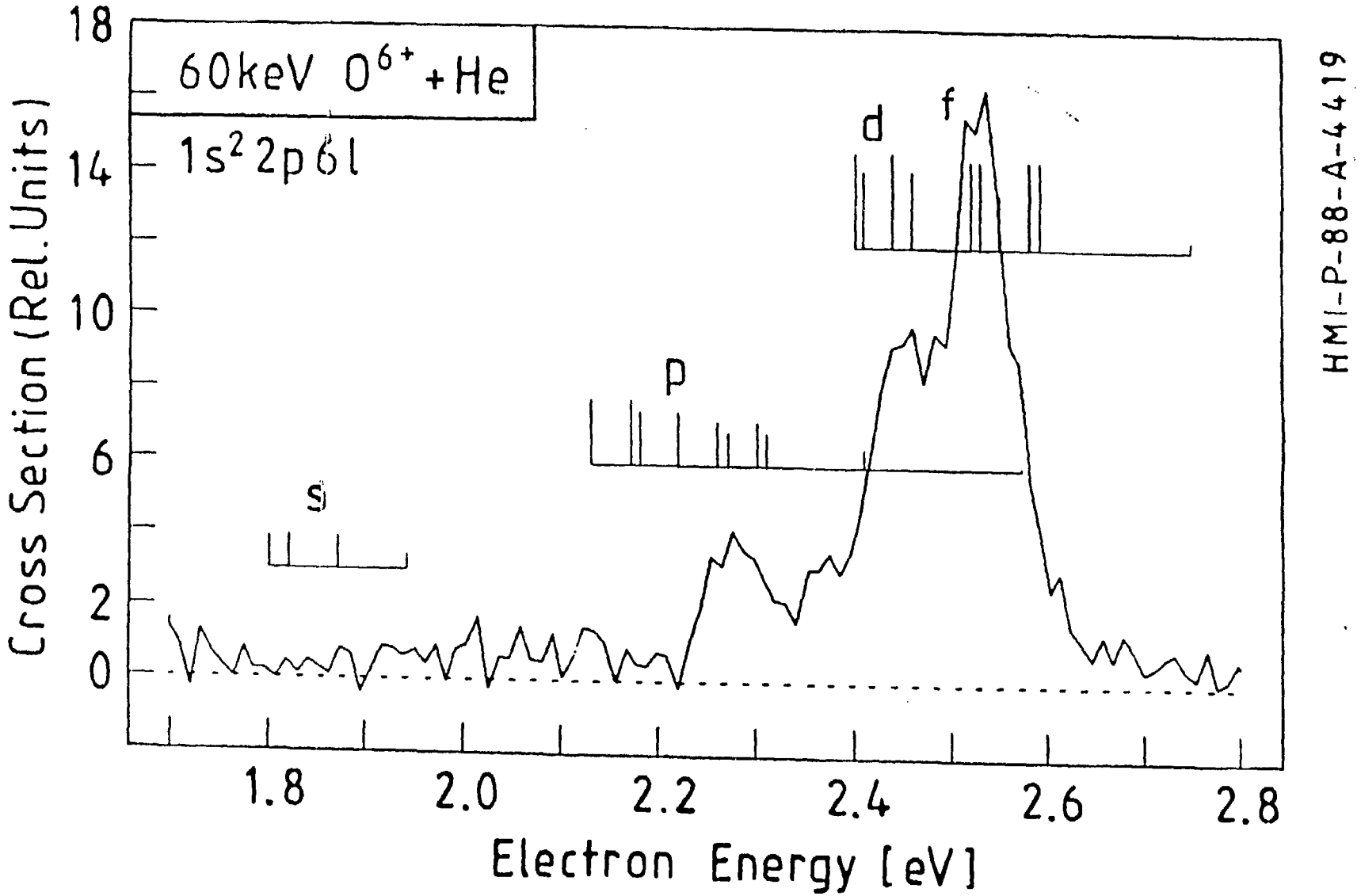

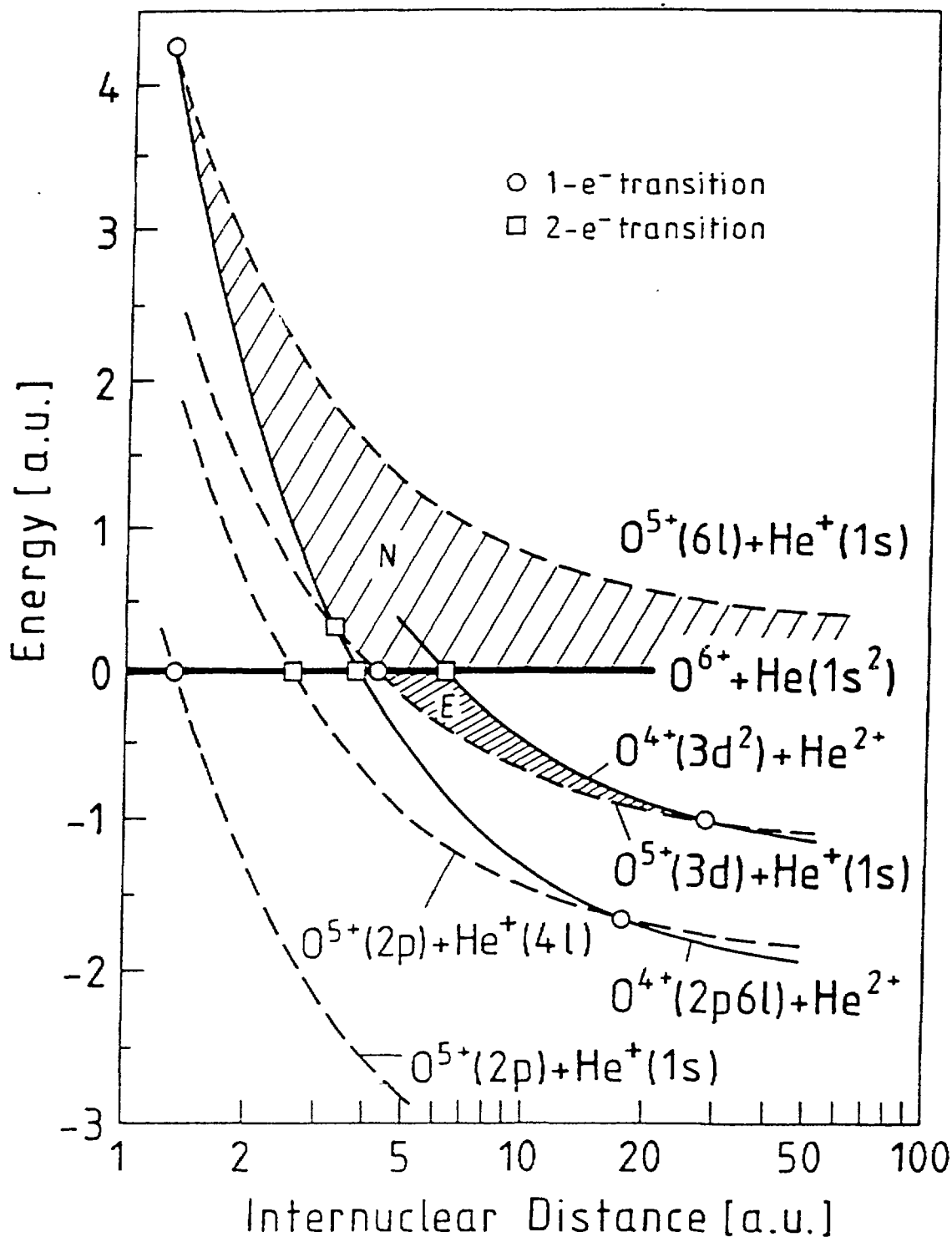
HMI-P-88-A-3322
○ 1-e⁻ transition
□ 2-e⁻ transition
Energy [a.u.]
Internuclear Distance [a.u.]
4
3
2
1
0
-1
-2
-3
1
2
5
10
20
50
100
N
E
O5+(6l)+He+(1s)
O6+ + He(1s2)
O4+(3d2)+He2+
O5+(3d)+He+(1s)
O5+(2p)+He+(4l)
O4+(2p6l)+He2+
O5+(2p)+He+(1s)

Fig. 4